nature photonics

SUPPLEMENTARY INFORMATION

DOI: 10.1038/NPHOTON.2012.332

Supplemental information: Experimental demonstration of optical transport, sorting and self-arrangement using a "tractor" beam

O. Brzobohatý[1], V. Karásek[1], M. Šiler[1], L. Chvátal[1], T. Čižmár[2] and P. Zemánek[1]

[1]*Institute of Scientific Instruments of the ASCR, v.v.i., Královopolská 147, 612 64 Brno, Czech Republic*

[2]*School of Medicine, University of St Andrews, North Haugh, Fife KY16 9SS, UK*

1 Theoretical simulations

1.1 Single spherical particle illuminated by two plane waves

We employed the generalized Lorenz-Mie theory (GLMT) [1, 2] to perform a parametric study of optical forces acting upon polystyrene spheres with refractive index 1.59 and radii bellow $a < 5\,\mu$m and illuminated by two interfering plane waves (vacuum wavelength 532 nm) with mutual tilt $0 \leq 2\theta_0 \leq 180°$. Particles were surrounded by water with refractive index 1.33. Depending on the particle radius a and the incident angle θ_0, the particle settles with its centre either in the intensity maximum or minimum [3]. Figure 1 presents the forces acting upon polystyrene particles smaller than $a < 1\,\mu$m; the blue and green colour-map denotes the particle confined in the intensity maximum and minimum of the interference fringe, respectively. The white curves mark combinations of parameters where the particle moves in the negative z direction, i.e. the pulling force exists. This figure demonstrates that for polystyrene particles with radii bellow $1\,\mu$m the pulling force exists only for s-polarized beams.

Figure 2 reveals incident angles $\theta_{0,\mathrm{min}}$ giving minimal force F_z (i.e. maximal pulling force) for polystyrene particles of radii up to $5\,\mu$m placed at their equilibrium positions. The results demonstrate that polystyrene particles with radii larger than $1\,\mu$m can be pulled against the z-axis also for p-polarized beams. Moreover, for certain particles sizes the amplitude of the

DOI: 10.1038/NPHOTON.2012.332

pulling force for p-polarized beams exceeds that for s-polarized.

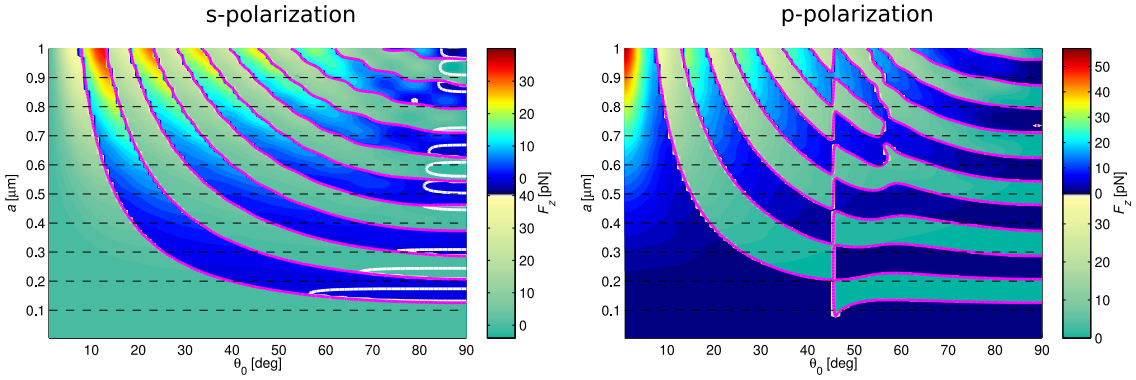

Figure 1: Optical force in z direction acting on a polystyrene particle as a function of the particle size a and the incident angle θ_0 of two interfering plane waves. The left and right figure corresponds to s-polarized and p-polarized wave, respectively. The forces are calculated for a particle located in its stable location with respect to the fringes of the standing wave. Different pseudo-colour maps correspond to the particle located in the standing wave intensity maximum (blue-red colour-map) or in the standing wave minimum (green colour-map). Cyan curves show combinations of tilt angles θ_0 and particle sizes where the particle motion across the fringes is not influenced by the standing wave. The white curves mark combinations of parameters where the particle moves in the negative z direction, i.e. the pulling force exists. Due to the chosen description of the incident field, the position of the standing wave nodes for p-polarized light and the incident angle $\theta_0 < 45°$ moves by a quarter of wavelength, i.e. from $y = 0$ to $y = \lambda/[4\sin(\theta_0)]$.

Based on our theoretical predictions we have chosen polystyrene particles of radii 410 nm and 1000 nm for our experiments as they are pulled against the k-vector within the tractor beam. To demonstrate the opposite case we have chosen polystyrene particles of radii 300 nm and 800 nm that are pushed along the direction of the resulting k-vector. Figures 3 and 4 present the GLMT calculations of the optical forces F_z and F_y acting upon a single polystyrene particle of radius 410 nm and 300 nm placed in two interfering s-polarized (top row) and p-polarized (bottom row) plane waves. The particle is located at different y positions across the fringe and all possible incident angles θ_0 are considered. According to Fig. 1f in the main text, polystyrene particles of radii 410 nm and 300 nm behave differently for s-polarized beams and incident angles $\theta_0 > 80°$, therefore they have been selected for the sorting experiments.

Figure 5 shows a scattering diagram of the field scattered by the polystyrene particle of radius 410 nm illuminated by two interfering plane waves with the incident angle $\theta_0 = \pm 86.25°$ towards the z-axis. The figure demonstrates that for s-polarized waves (red curve), in contrast to p-polarized waves (blue curve), the forward scattering is slightly more enhanced towards the polar angles lower than the incident angle ($\langle\theta\rangle < \theta_0$) which causes the pulling force.

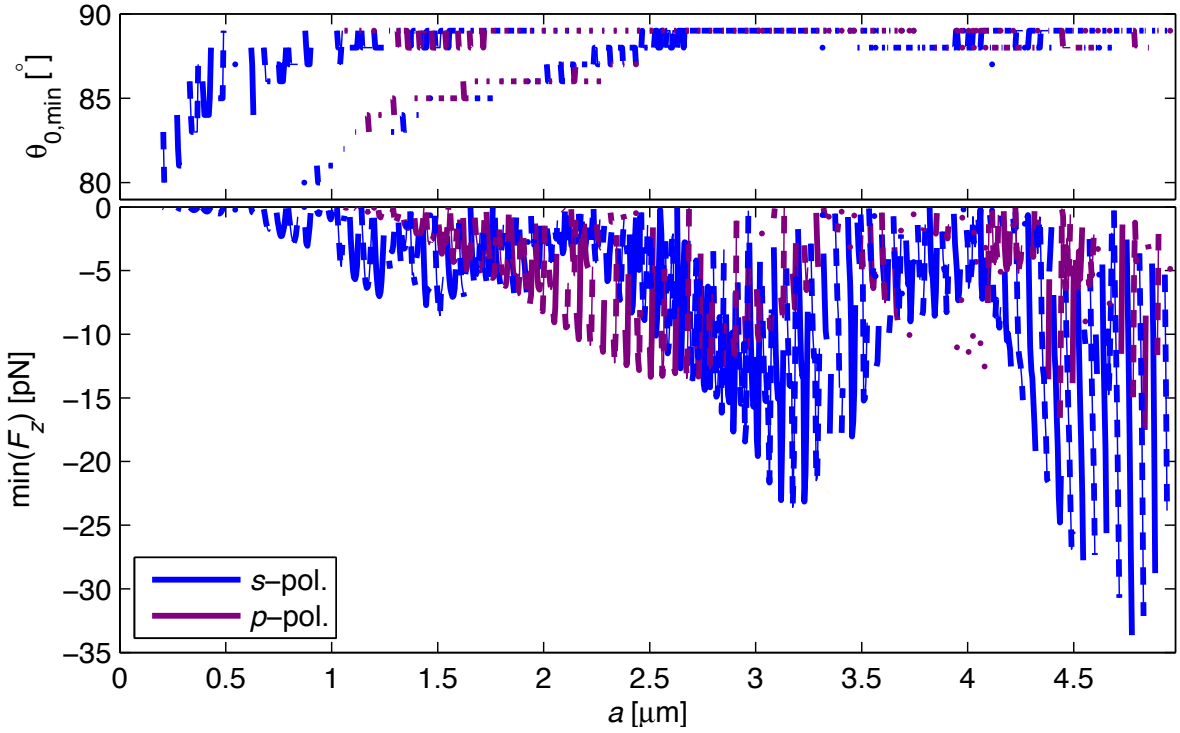

Figure 2: Incident angles $\theta_{0,\min}$ giving minimal force F_z (i.e. maximal pulling force) displayed for polystyrene particles of different radii. Polystyrene particles with radii larger than 1 μm can be pulled also by p-polarized beams.

Figure 6 demonstrates asymmetric scattering with respect to the plane of incidence for orientation of the incident polarization of $\psi = 0°$, $\pm 45°$ and $90°$. This asymmetric scattering leads to the particle motion in the direction perpendicular to the plane of incidence (along x-axis). If the optical force acting upon the particles is calculated, Fig. 7 demonstrates the periodic dependences of such optical force components F_x and F_z in the $x - z$ plane on the angle ψ of the linearly polarized plane waves.

DOI: 10.1038/NPHOTON.2012.332

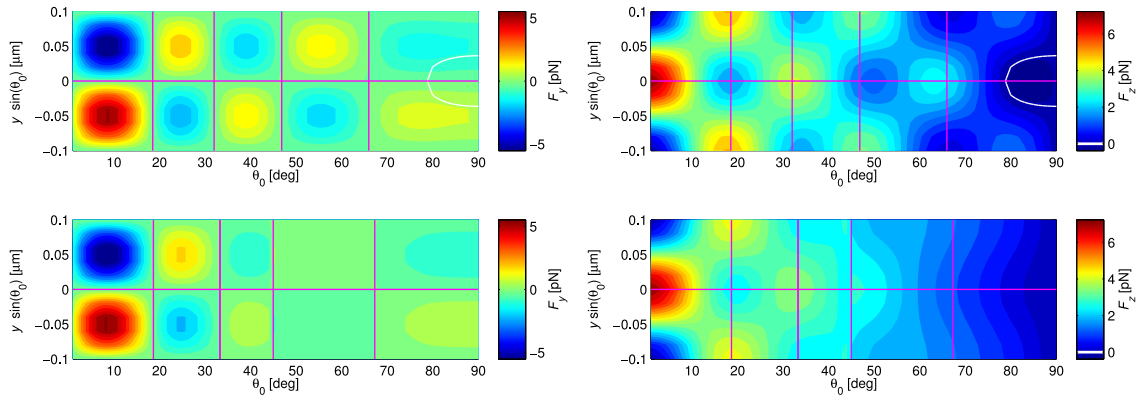

Figure 3: Examples of the GLMT calculations of the optical forces F_z and F_y acting upon a single polystyrene particle of radius 410 nm placed in two interfering s-polarized (top row) and p-polarized (bottom row) plane waves. The particle is located at different y positions across the fringe and all possible incident angles θ_0 are considered. The region of the existence of the pulling force F_z is only inside the white curve denoted for s-polarized beam where the particle is confined with its centre in the fringe intensity maximum located at $y = 0$. Red lines denote the positions where the force F_y across the fringes is equal to zero.

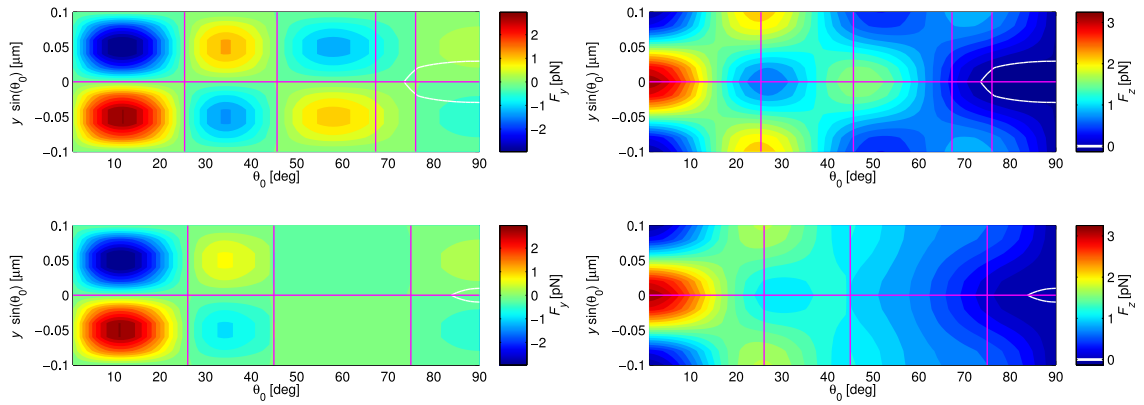

Figure 4: Examples of the GLMT calculations of the optical force F_z and F_y acting upon a single polystyrene particle of radius 300 nm placed in two interfering s-polarized (top row) and p-polarized (bottom row) plane waves. The particle is located at different y positions across the fringe and all possible incident angles θ_0 are considered. The region of the existence of the pulling force F_z is only inside the white curves, but here the fringe intensity maximum located at $y = 0$ represents the unstable position for angles close to 90°. For $\theta_0 > 76°$ such particle will not experience the pulling force if settled stably in the fringes. However, for s-polarized beam incident under $72° < \theta_0 < 76°$ the particle is stably trapped at $y = 0$ and negative F_z exists pulling it against the direction of the z-axis. Red lines denote the positions where the force F_y across the fringes is equal to zero.

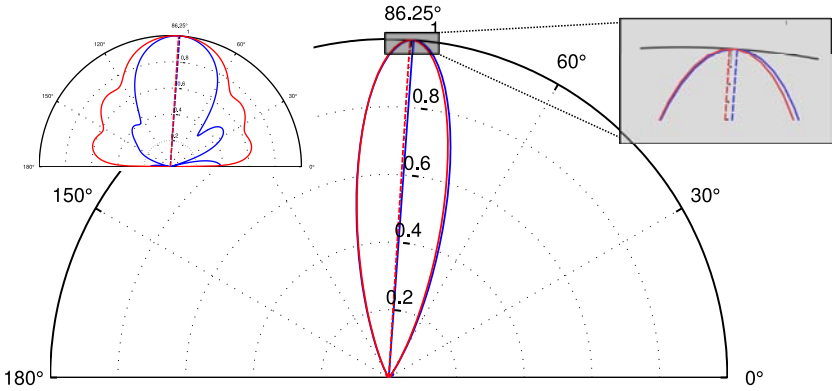

Figure 5: Calculated scattering diagram for a polystyrene particle of radius 410 nm illuminated by two plane waves incident at $\theta_0 = \pm 86.25°$ (due to the symmetry only one half-space is shown). The blue or red curve corresponds to s-polarized or p-polarized beam, respectively. The inset on the left-hand side shows the scattering diagram plotted in logarithmic scale and slightly enhanced forward scattering (i.e. towards smaller polar angles) is visible for s-polarized beam.

DOI: 10.1038/NPHOTON.2012.332

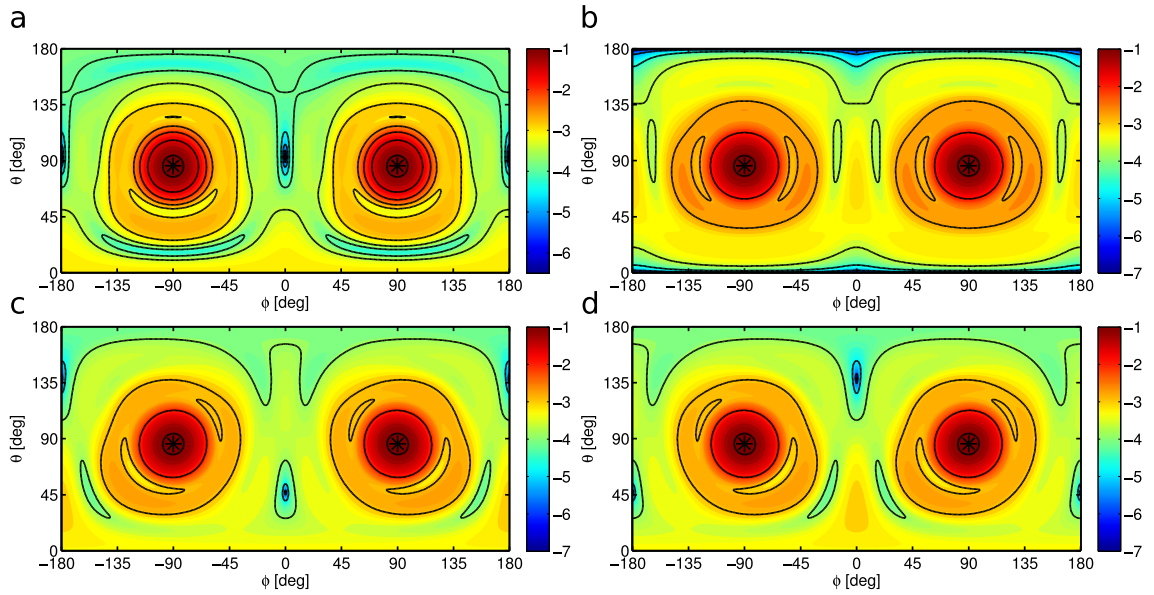

Figure 6: Far-field optical intensity of the light scattered by a polystyrene sphere of radius 410 nm plotted as the function of the azimuthal ϕ and polar θ angles. The optical intensity is shown in logarithmic scale and normed to its maximal value for each case. **a,** The image denotes the case for s-polarized incident plane waves. It correspond to $\psi = 0$ and the components of the intensity of the electric field are equal to $\mathbf{E}_1 = (|\mathbf{E}_1|, 0, 0)$, $\mathbf{E}_2 = (|\mathbf{E}_2|, 0, 0))$. **b,** This case corresponds to p-polarized waves with $\psi = 90°$ and $\mathbf{E}_1 = (0, |\mathbf{E}_1|\cos(\theta_0), |\mathbf{E}_1|\sin(\theta_0)$, $\mathbf{E}_2 = (0, -|\mathbf{E}_2|\cos(\theta_0), |\mathbf{E}_2|\sin(\theta_0))$ incident plane waves. Light scattering towards polar angles θ lower that the incident angle (θ_0) causes the pulling force (e.g. for s-polarized incident waves). The scattering diagram is symmetrical with respect to the azimuthal angle $\phi = \pm 90°$ (corresponding to the plane of incidence) and, therefore, no optical force occurs along x-axis. The bottom row corresponds to the linear polarization $\psi = 45°$ (**c,**) or $\psi = -45°$ (**d,**) with corresponding electric field intensities $\mathbf{E}_1 = (|\mathbf{E}_1|\cos(\psi), |\mathbf{E}_1|\cos(\theta_0)\sin(\psi), |\mathbf{E}_1|\sin(\theta_0)\sin(\psi))$, $\mathbf{E}_2 = (|\mathbf{E}_2|\cos(\psi), -|\mathbf{E}_2|\cos(\theta_0)\sin(\psi), |\mathbf{E}_2|\sin(\theta_0)\sin(\psi))$, respectively. Asymmetric scattering with respect to the plane of incidence leads to the force component in x direction which causes particle motion in $x - z$ plane as observed in Figs 2 and 4 in the main text. The directions of the incident plane waves are denoted by $*$.

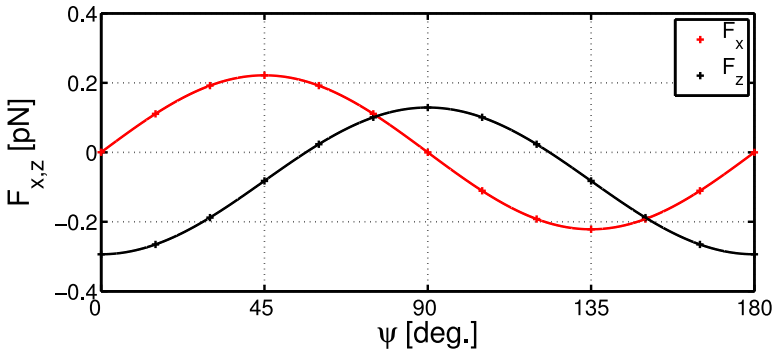

Figure 7: Optical forces F_x and F_z acting upon a polystyrene particle of radius 410 nm calculated for the case of two interfering plane waves described in Fig 6 as a function of the polarization ψ. We assumed the incident angle $\theta_0 = \pm 86.25^\circ$ and the optical intensity equal to $1.77\,\mathrm{mW}/\mu\mathrm{m}^2$.

DOI: 10.1038/NPHOTON.2012.332

1.2 Single spherical particle in Gaussian beams

In the experimental realization of the "tractor" beam we employed a wide Gaussian beam that was retro-reflected on a mirror thus substituting two interfering plane waves described above. The optical force originating from the Gaussian intensity profile along the z-axis attracts the particles toward the centre and so acts against both, the pulling or the pushing forces (as it was explained in Figs. 2a,b,c of the main text). Therefore, if the beam is switched on or its polarization is changed, the pulling or pushing forces propel the particles to their new equilibrium positions established in the Gaussian beams. To develop an appropriate theoretical description of the geometry we need to take into account not only the Gaussian beam intensity profile, dragging particles to the beam centre, but also the influence of the scattered field reflected on the mirror back towards the particle [4]. The results of our calculations (see Fig. 2c of the main text) show that the reflection of the scattered field on the mirror does not significantly influence the resulting optical force.

Figure 8 shows the results of such theoretical simulations in the form of particle trajectories in the $y-z$ plane for several starting positions for each of the considered polarization (s and p) and particle radius (410 nm and 300 nm). For p-polarized beams particles of both radii 300 nm and 410 nm are not confined in the standing wave and move along positive direction of the y-axis, i.e. towards the top coverslip. However, for s-polarized beams the 410 nm particle moves against the z-axis well localized near the standing wave intensity maximum and finally reaches its equilibrium position near $z = -10\,\mu$m. The behaviour of the 300 nm particle is more complex because only particles started at distinct positions reach an attractor-like trajectory around $z = 10\,\mu$m and stay localized in the standing wave fringe. Particles initially placed farther at the positive part of the z-axis are attracted towards the beam centre but travel across the fringes towards the top surface. The colour of the trajectories encodes the particle speed at the given position. This results coincide with our experimental observations.

If we extended our stability investigations into 3D and for more beam polarization angles ψ, we obtained equilibrium positions shown in Fig. 9. The particle of radius 410 nm is not confined in the fringes along y direction (for comparison see Fig. 8) which coincides with observed experimental trends. However, slightly larger particle of radius 420 nm stayed confined for all polarizations.

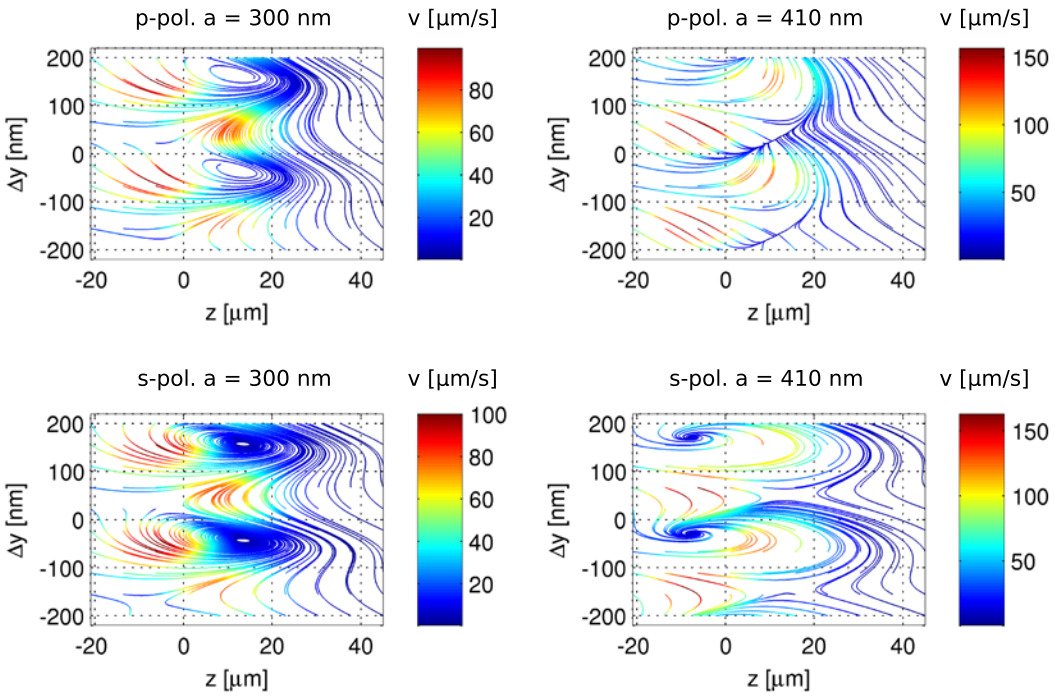

Figure 8: Calculated trajectories of a single polystyrene particle in the $y-z$ plane corresponding to different initial positions. Optical forces acting along the z-axis and the y-axis upon a single polystyrene particle of radii 300 nm, and 410 nm were calculated using coupled dipoles. Particles are placed 45 μm above the mirror surface and illuminated by the incident and the reflected s-polarized or p-polarized Gaussian beam. Calculated optical forces in this overdamped system were used to determine the trajectories of particles started initially at various positions in the beam without considering the thermal disturbance of the surrounding medium. The colour of the curves encodes the particle velocity at given position. The Gaussian beam waist was placed on the bottom reflective coverslip and was equal to $w_0 = 23.5\,\mu$m, the total incident beam power was 3.2 W.

DOI: 10.1038/NPHOTON.2012.332

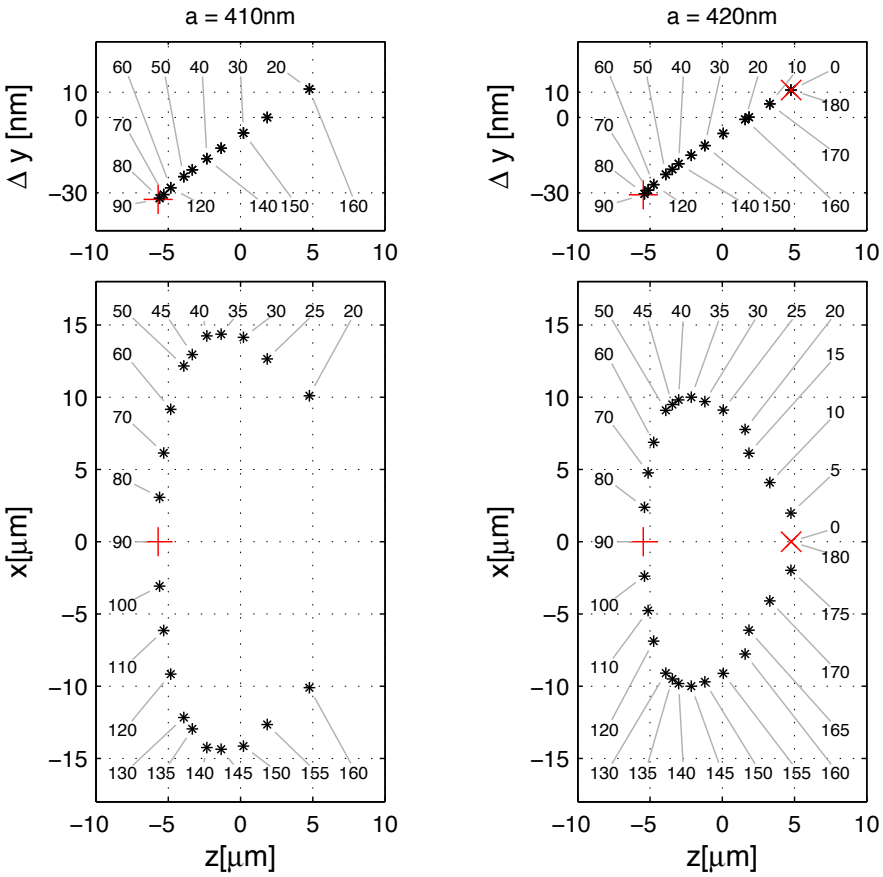

Figure 9: Stable positions of polystyrene particle of radius 410 nm and 420 nm calculated using coupled dipoles approximation. The particle is illuminated by the retro-reflected Gaussian beam of waist radius $w_0 = 23.5\,\mu$m and its polarization ψ varied between 0° and 180°. The particle is trapped 45 μm above the mirror surface and slight deviations of its equilibrium positions from an intensity maxima of the standing wave is observed. It is seen that the theory does not predict stable trapping of 410 nm particles along the y-axis for p-polarized beams. However, further investigations show that slightly larger particle of radius 420 nm is stably trapped in y direction also for p-polarized beam (right part of the figure). Red + or × marks denote the stable positions of the particle illuminated by s-polarized or p-polarized beam, respectively.

2 Experimental observations

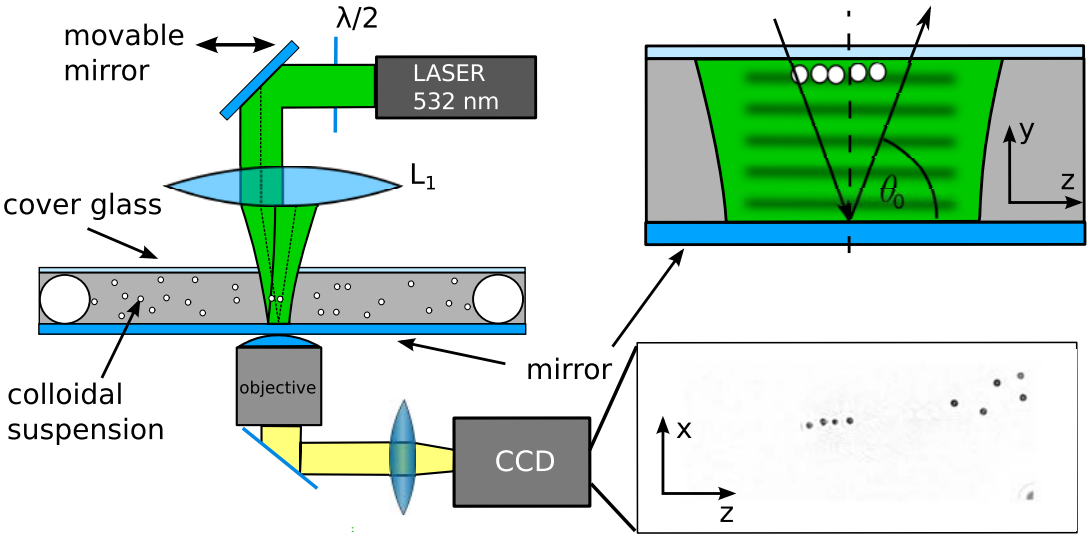

Figure 10: Experimental set-up. The Gaussian beam was emitted from VERDI V5 (Coherent; vacuum wavelength 532 nm) and was reflected at the horizontally movable mirror (along the z-axis) that directed the beam through a lens L_1 of focal length 150 mm. Position of the beam centre at the lens determined the incident angle θ_0 and it was controlled by the position of the mirror. The beam passed through the suspension of dielectric spheres (Duke Scientific) placed between two coverslips. The bottom coverslip was coated with a system of dielectric layers retro-reflecting 99% of the incident beam. The beam was focused to the beam waist $w_0 = 23.5\,\mu$m placed on the reflecting coverslip. In the case of the beam waist $w_0 = 39\,\mu$m, a demagnifying telescope made of lenses of focal lengths 150 mm and 200 mm was used (not shown in the figure). The interference of the incoming and reflected beams created a standing wave along the y-axis over the distance between the coverslips that was set by the polystyrene spheres of diameter 50 μm. The suspension of microparticles was observed through microscope objective (Olympus 100x, oil) at the CCD camera (Basler GigE).

When a suspension of dielectric spheres was put into the sample, the particles illuminated by the beams with certain incident angles self-organized but they were not in contact, see Fig. 10.

Figures 11 and 12 demonstrate different types of optically bound structures that were created in the Gaussian beam. In the case of s-polarization, the light is strongly scattered along the z-axis and, therefore, the optically bound structures are elongated along the z-axis – as Fig. 11 shows. In the case of p-polarized beams particles scatter strongly along the x-axis and, therefore, the optically bound structures tend to be more tightly organized along this axis. We observed that in contrast to the single particle, the optically bound polystyrene particles of radii 410 nm experience pulling force not only for s-polarized light but also for p-polarized light. Figures 11 and 12 show stable configurations of optically bound structures pulled against the beams

DOI: 10.1038/NPHOTON.2012.332

propagation for s- and p-polarized Gaussian beams with the beam waist 23.5 μm.

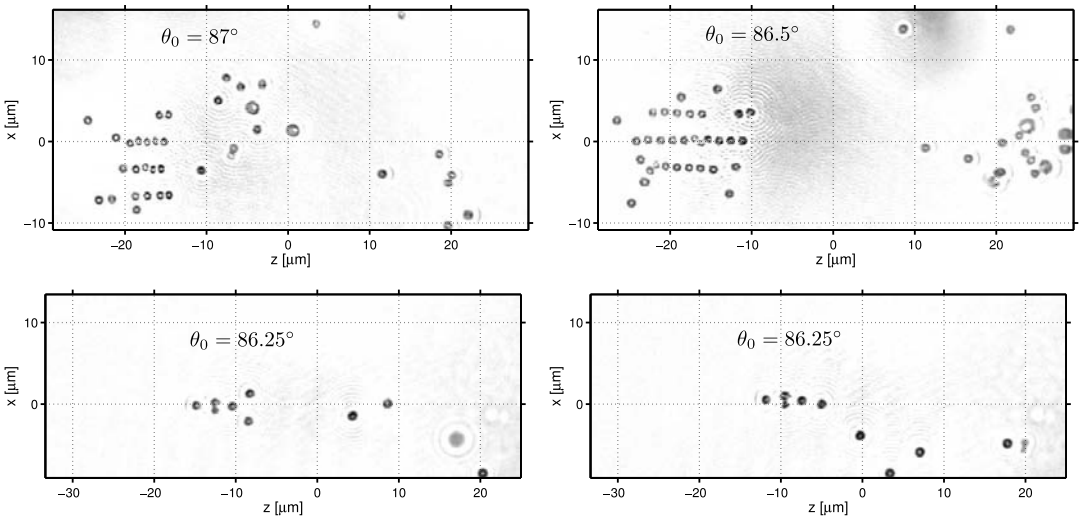

Figure 11: s-polarization: examples of several optically bound structures composed of polystyrene particles of radius 410 nm and created 25μm above the mirror (in this case 25 μm polystyrene spheres were used as spacers). Incident laser power was 3.2 W and beam waist $w_0 = 23.5\,\mu$m.

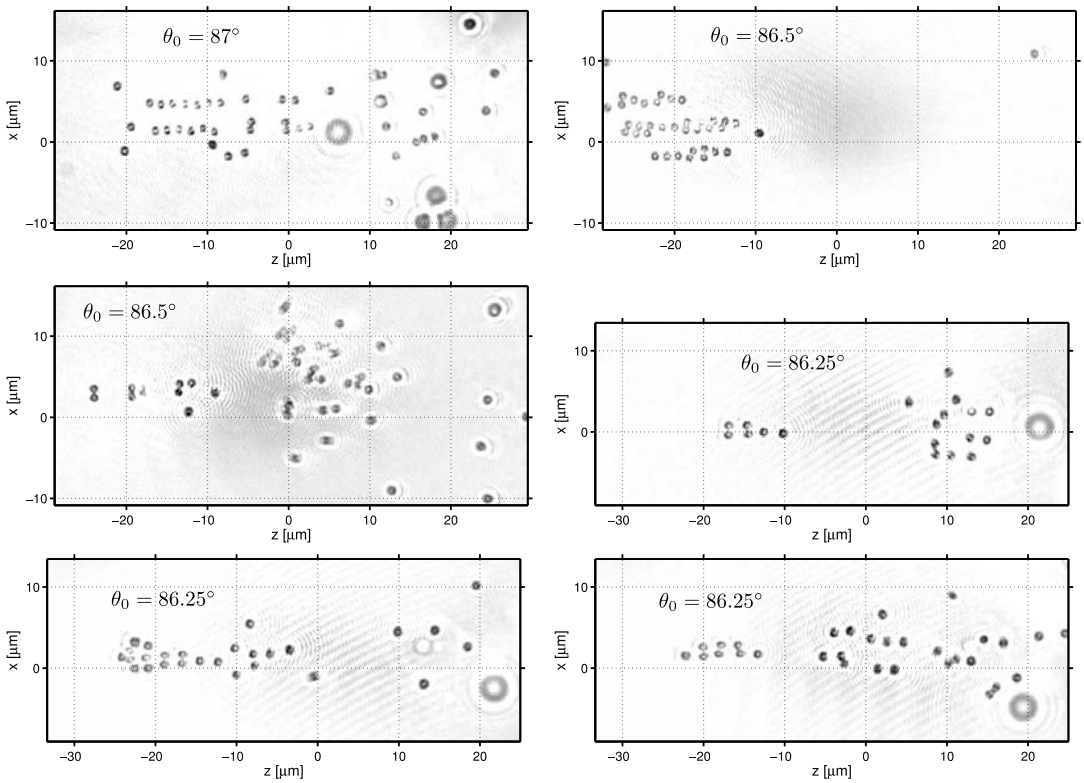

Figure 12: p-polarization: examples of several optically bound structures observed under the same remaining conditions as in Fig. 11.

DOI: 10.1038/NPHOTON.2012.332

Figure 13 illustrates strong influence of the organization of the particles in the cluster on their behaviour. At the beginning the suspension of disorganized individual particles is illuminated by s-polarized beam and the particles are pulled by the "tractor" beam to the region $-27\,\mu\text{m} \leq z \leq -24\,\mu\text{m}$ where they stayed near the bottom coverslip. If the beam polarization is slowly changed to p-polarization, particles formed optically bound structures oriented along the x-axis localized at the region $-13\,\mu\text{m} \leq z \leq -10\,\mu\text{m}$ and stayed still near the bottom coverslip. The structure is evidently under the influence of the pulling force even for p-polarized beam. However, if the polarization is switched too fast from the initial s-polarization to p-polarization, the particles of radius 410 nm move upwards to the upper coverslip (50 μm above the mirror) and tend to be rather disorganized, more separated from each other, and localized between $20\,\mu\text{m} \leq z \leq 30\,\mu\text{m}$.

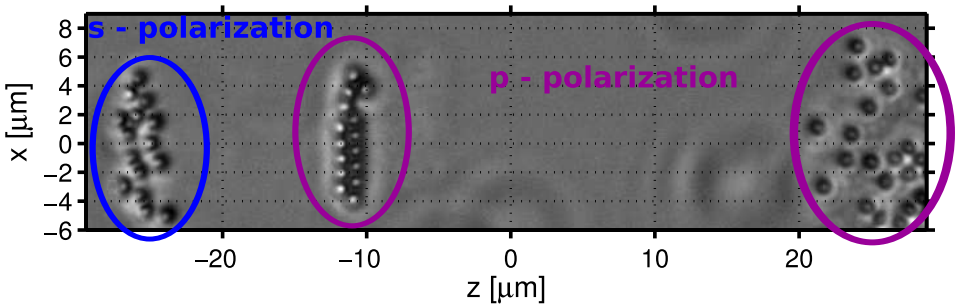

Figure 13: Different behaviour of polystyrene particles of radii 410 nm initially illuminated by s-polarized "tractor" beam (structure in the blue ellipse). If the beam polarization is slowly changed to p-polarization, the same particles optically self-organized into the structure in the middle and stayed close to the bottom coverslip. However, fast transition to the p-polarization caused particles movement towards the top coverslip and formation of disorganized structure shown in the right. The following beam parameters were used: beam waist $w_0 = 39\,\mu\text{m}$, incident power 3.2 W, and incident angle $\theta_0 = 86.25°$.

References

[1] Barton, J. P., Alexander, D. R. & Schaub, S. A. Theoretical determination of net radiation force and torque for a spherical particle illuminated by a focused laser beam. *J. Appl. Phys.* **66**, 4594–4602 (1989).

[2] Gouesbet, G., Lock, J. & Grehan, G. Generalized Lorenz-Mie theories and description of electromagnetic arbitrary shaped beams:localized approximations and localized beam models, a review. *J. Quant. Spectr. & Rad. Transfer* **112**, 1–27 (2011).

[3] Zemánek, P., Jonáš, A. & Liška, M. Simplified description of optical forces acting on a nanoparticle in the gaussian standing wave. *J. Opt. Soc. Am. A* **19**, 1025–1034 (2002).

[4] Brzobohatý, O. *et al.* Experimental and theoretical determination of optical binding forces. *Opt. Express* **18**, 25389–25402 (2010).